An Approach to Separating Pu, U, and Ti from High-Purity Graphite for Isotopic Analysis by MC-ICP-MS

Shalina C. Metzger*, Benjamin T. Manard, Debra A. Bostick, Brian W. Ticknor, Kayron T. Rogers, Eddy H. McBay, David C. Glasgow, N. Alex Zirakparvar and Cole R. Hexel

Chemical Sciences Division, Oak Ridge National Laboratory, Oak Ridge, TN, 37830

*Corresponding author: MetzgerSC@ornl.gov

Abstract

Information about elemental and isotopic systematics of ultra-trace level actinides (e.g. U and Pu) and main group elements (e.g. Ti) present within nuclear grade graphite is vital to the nuclear community for improved reactor operation and security. In support of this, extensive effort has been placed on improving analysis methods (i.e., inductively coupled plasma – mass spectrometry). However, significantly less effort has been devoted to the optimization of chemical separation methods. Within the separation community, commercially available Eichrom™ resins are often employed, as their elution characteristics for various elements have been well studied, but the direct optimization of actinides and trace metal separations from a single sample have not been widely investigated. Here, methods using various Eichrom pre-packed cartridges were explored to achieve separation of ultra-trace levels of U, Pu, and Ti from a variety of graphite samples. Once the validity of the combined separation scheme was established using certified reference materials, the method was applied to historic, unirradiated and irradiated, graphite samples. For all samples investigated, precise isotope ratio measurements for the titanium isotope systems were made.

Keywords: Uranium; Plutonium; Titanium; MC-ICP-MS; Graphite; Separations

Graphite has a wide range of applications, and a portion of the 1.1 million metric tons of graphite mined in 2019[1] was utilized for neutron moderation in nuclear reactors. Graphite is an excellent material for this purpose due to its very low neutron absorption cross section and good thermalization properties which allows fast neutrons to be slowed down without losing them to capture.[2] As fission is more likely at lower neutron energies, many reactor designs require neutrons to be slowed down, or 'moderated', to energies in the thermal equilibrium range (~0.025 eV) to increase the probability of fission.[3] The first implementation of a graphite moderated reactor (GMR) was successfully demonstrated in the 1940s (Chicago Pile-1) and was made with > 300 metric tons of nuclear grade graphite.[4] Graphite suitable for use in nuclear reactors (e.g. nuclear grade graphite) is purified through thermodiffusion and chemical purification techniques, or through the process of graphitization with special care taken to minimize certain impurities.[2] Despite purification efforts, ultra-trace level impurities do remain, and vary based on the production process for each batch and factory.[5] Some elements (i.e., Ti) remain after purification as ubiquitous impurities due to their resistance to thermal refinement techniques. Therefore, the

analysis of trace element impurities is crucial for manufacturers to consistently produce reliable material. It is important to note that the impurities in the graphite could have an effect on its moderation capability. As such, research has been done to help develop characterization methods for various graphite materials.[6-13]

Many techniques have been employed for the quantification of trace elements in graphite. Two widely utilized techniques are solution-based inductively coupled plasma - optical emission spectroscopy / mass spectrometry (ICP-OES/MS). Both typically require complete digestion of the sample, which has been accomplished using various lengthy multi-step dissolution protocols aimed at providing a homogeneous sample.[5-9, 14, 15] Laser ablation (LA) coupled to ICP-MS can provide spatially resolved impurity data[10, 16], and does not require sample digestion; however, the technique lends itself to variability within a sample due to spot-to-spot differences which can be further hindered by the heterogeneity of graphite.[10] Other viable techniques have been explored to directly analyze the sample including charged particle activation analysis (CPAA)[13], neutron activation analysis (NAA) techniques[5, 13, 17], X-ray fluorescence spectrometry[18], as well as glow discharge atomic absorption spectrometry[19]. However, while these techniques determined the concentration of trace elements at μg g^{-1} and ng g^{-1} levels in various graphite samples, the isotopic composition was not reported.

Several trace impurities in graphite (i.e., B, Ti, and U) have higher thermal neutron cross sections and are more likely to react with neutrons during reactor operation. The thermal neutron cross section is an attribute specific to each isotope and is a measure of the interaction probability of a nucleus with neutrons over a range of neutron energies. For example, ^{10}B has a higher neutron cross section than ^{11}B (0.3 barns [n,γ] and 0.005 barns [n,γ], respectively), and ^{10}B can undergo additional neutron capture reactions (3,840 barns [n,α]). As such, ^{10}B will react with significantly more neutrons than ^{11}B and the natural $^{10}B/^{11}B$ isotope ratio will be perturbed. Similarly, ^{46}Ti, ^{47}Ti, ^{48}Ti, ^{49}Ti, and ^{50}Ti all have different cross sections (0.6, 1.7, 7.9, 1.9, and 0.177 [n,γ] respectively) and will react in predictable ways during irradiation causing a perturbation in their isotope ratios. It is assumed that any impurities within the graphite are present initially in their natural isotopic abundances. As the graphite reactor operates, thermal neutrons can react with impurities that have higher neutron cross sections resulting in perturbed isotope ratios for those elements. This change in the isotopic composition of the impurities can provide information about the overall energy production of the reactor during operation.[20] Multi-collector-ICP-MS (MC-ICP-MS) and thermal

ionization-MS (TIMS) are typically utilized for isotopic ratio measurements due to the fact that they afford the high level of analytical sensitivity and precision that is necessary to accurately determine isotopic variations in trace and ultra-trace level elemental impurities.[21-27]

One requirement for precise isotope ratio measurements is the need to remove interferences, both molecular and isobaric, prior to analysis.[28] As MC-ICP-MS is widely used in nuclear safeguards applications for U and Pu isotopic measurements, extensive research has been done on the separation of U from Pu to resolve isobaric and molecular interferences.[22-25, 29-31] In comparison, Ti isotope ratio measurements have faced drawbacks due to mass dependent fractionation along with molecular and isobaric interferences (e.g., ^{46}Ca, ^{48}Ca, ^{50}V, ^{50}Cr) that have proved difficult to fully separate chemically, and resolve mass spectrometrically.[27, 32-34] Further complicating the measurements are relatively large uncertainties on the available Ti reference materials which use the International Union of Pure and Applied Chemistry (IUPAC) Ti isotope abundances.[35] Ideally, a Certified Reference Material (CRM) with certified Ti isotope ratios would improve the uncertainty.[36] A recent study on Ti isotope ratios in geological samples using MC-ICP-MS utilized a double spike method to increase the precision of the measurement by quantifying the change in the samples compared to a reference material.[37] While precise differences in the ratio were accurately identified, the method required extensive column separation to remove interferences (e.g., ^{48}Ca on ^{48}Ti) from the geological sample.[28] Several methods for geological Ti separations have been reported[34, 37-40], but it is unclear if the adaptation of separation schemes from geological samples to graphite samples would be valuable. This ambiguity is driven by the overall quantity of Ti in typical geological samples (high μg g^{-1} to low mg g^{-1}) compared to graphite samples (<100 ng g^{-1} to low μg g^{-1}), with nuclear grade graphite expected to be even lower.[6-10, 13] As such, the low procedural blanks (4-20 ng natural Ti) previously observed,[34] which did not affect the isotope ratio measurements of natural Ti in geological samples, may affect the measurement of Ti isotopes in graphite. Therefore, the investigation of how to separate Ti from other trace elements at very low levels is warranted

Here, the separation of U, Pu, and trace elements (Ti) from a graphite sample for isotope ratio measurements using commercially available resins is presented. The separated elements were then analyzed using MC-ICP-MS for isotope ratio measurements with the overall goal of achieving low expanded uncertainties. After optimizing the individual separations, simulated samples containing a U and Pu CRM and a known Ti enriched spike were separated as an initial proof of

concept study. Mixed element standards were used to evaluate the method for possible interferences. Successful separation of several interferences on the chosen elements (Ti, U, and Pu) was achieved enabling high precision MC-ICP-MS measurements which were in good agreement with the expected values. Separation of the selected elements from unirradiated graphite samples was completed and yielded natural isotope ratios via MC-ICP-MS, as expected. Additionally, blind graphite samples that had been previously characterized for U and Pu were successfully separated and measured. The isotope ratio measurements for U and Pu were in good agreement with the expected values. The Ti isotope ratios showed a significant difference between the unirradiated and irradiated graphite samples.

Experimental

Reagents and Standards

Optima™ grade reagents (HNO_3, HF, HCl, and H_2O_2 [30%],) were purchased from Fisher Scientific (Pittsburg, PA) and used without further purification. $NaNO_2$ (ACS, 95% min) and $FeSO_4$ Puratronic® 99.999% (metals basis) were purchased from Alfa Aesar (Tewksbury, MA). Multielement standard ICP-MS-68B-A and ICP-MS-68B-B containing 48 and 13 elements at 100 μg g^{-1} and a single element standard of Ti at 10 μg g^{-1} were purchased from High Purity Standards (North Charleston, SC) and used without further purification. CRMs for Pu and U were purchased from the New Brunswick Laboratory Program Office (Oak Ridge, TN) [NBLPO 137 (Pu), NBLPO U010 (U)], or the Joint Research Center of the European Commission (Geel, Belgium) [IRMM–183 (U), IRMM–86 (Pu)]. A National Institute of Standards and Technology (NIST) Standard Reference Material (SRM) 3162a (Ti) was used without further purification. An enriched ^{47}Ti stable isotope sample was obtained from the National Isotope Development Center at Oak Ridge National Laboratory and analyzed for trace metal content and isotopic ratios prior to separation. ASTM Type I (18.2 MΩ–cm) water was generated with a Thermo Scientific (Waltham, MA) Barnstead GenPure xCAD Plus water purification system and was used to prepare all solutions. All labware was acid leached overnight at 60°C in sequential baths of 6 M HCl, 8 M HNO_3, and Type I water prior to use unless otherwise noted. TEVA and UTEVA (1 mL, 50-100 μm), DGA-Normal (2 mL, 50-100 μm), and Anion Exchange (1-X8, Chloride form) (2 mL, 100-200 mesh) prepacked cartridges were purchased from Eichrom Industries (Lisle, IL). Separations were

performed with the assistance of a Visiprep DL vacuum box system (Supelco, St. Louis, MO). Crystalline flake graphite (Alabama graphite, Lot: 2017-1) was purchased from the Alabama Graphite Corporation (Coosa County, AL) and used without further purification.

Instrumentation

Trace elemental analysis was performed on an inductively coupled plasma-optical emission spectrometer (ICP-OES) and/or mass spectrometer (-MS). For the ICP-OES, a Thermo Scientific (Bremen, Germany) iCAP 7400 was employed which was equipped with an Echelle spectrometer and charge injection device (CID) detector. The samples were introduced by means of an Elemental Scientific Inc. (ESI) SC-2DX autosampler at 800 μL min^{-1} into a quartz low flow nebulizer integrated with a quartz cyclonic spray chamber. For samples which required lower detection limits and isotopic screening, a Thermo Scientific sector field (SF) ICP-MS (Element 2) was utilized. Again, an SC-2DX autosampler was used with a self-aspirating (100 μL min^{-1}) nebulizer housed within a stable sample introduction (SSI) dual quartz spray chamber cooled by a PC^3 Peltier cooler to improve measurement precision. Measurements were made in low ($m\ \Delta m^{-1}$ <300) and medium resolution ($m\ \Delta m^{-1}$ >4000) modes depending on the element of interest.[41]

The isotopic composition of the purified U and Pu fractions was analyzed with a Neptune Plus (Thermo Instruments, Bremen, Germany) double-focusing MC-ICP-MS, equipped with ten faraday collectors, three secondary electron multipliers (SEM), and two compact discreet dynodes (CDD). Both the U and Pu sample analyses were performed in low resolution mode ($m\ \Delta m^{-1}$ = 300). The instrument was fitted with a jet interface for increased pumping capacity, a nickel jet sample cone, and a nickel X skimmer cone. The samples were aspirated using a 50 μL min^{-1} self-aspirating nebulizer with an Apex Omega high efficiency introduction system (ESI, Omaha, NE). All data for the samples were collected in static mode. During the U analysis, a 10^{-13} ohm amplifier resistor was used on the 235 mass faraday detector, a 10^{-11} ohm on the 238 mass, and for the minor isotopes, 234 and 236 were measured with SEMs. Plutonium was analyzed using a combination of CDDs and SEMs. The 239 mass was on CDD, and 240, 241, and 242 were on SEMs. The 238 mass for hydride correction was determined in a second data line with 238 on L5 faraday cup equipped with a 10^{-13} ohm amplifier resistor. The analysis sequence for both elements used a standard sample bracketing method with quality control samples dispersed after every third sample. The mass fractionation corrections were applied by direct comparison to an isotopic

reference material; NBLPO U010 for U and NBLPO 137 for Pu. The sample fractions were corrected for instrument blank and hydride contribution.

The Ti isotopic abundance was determined with a Neptune (Thermo Instruments, Bremen, Germany) double-focusing MC-ICP-MS, equipped with nine faraday collectors and one SEM. The instrument was equipped with a smaller slit, 16 μm, to increase the resolution modes compared to the standard slit, 50 μm ($m\ \Delta m^{-1}$ = ~4100). Samples were aspirated using a 100 μL min^{-1} self-aspirating nebulizer with a quartz stable sample introduction (SSI) cyclonic double pass spray chamber (ESI, Omaha, NE). All Ti isotopic data was collected in static mode on faraday cups using 15 cycles each with 8.389 s integration time per cycle. The 46, 47, and 48 masses were configured with 10^{-11} ohm amplifier resistors and 10^{-13} ohm resistors were utilized for mass 49 and 50. The analysis sequence used a standard sample bracketing method with quality control samples dispersed after every sample. Ti sample solutions were screened to determine the Ca, V, and Cr isobaric interference contributions before analysis. If present in the screen, the interfering element was quantified by measuring one of its non-interfering isotopes. Assuming natural abundance, this then allowed for the counts of the Ti isotope to be corrected on an individual isotope basis by subtracting counts of the interfering element. The addition of up to 1 mg of carbon did not demonstrate an interference on the ^{50}Ti isotope. Mass fractionation was corrected using direct comparison, and verified using an exponential equation, to a comparator sample. The comparator standard was NIST SRM 3162a standard solution, and the IUPAC natural isotopic composition was applied for the ratio values.

Uncertainty

The expanded uncertainty (U_C) for the isotope ratio measurements were calculated using methods compliant with the Guide to the Uncertainty in Measurement (GUM) with a coverage factor of 2 (k = 2) unless otherwise stated.[42] Equation 1 was used as the model equation in the GUM Workbench® for the evaluation of expanded uncertainties for the isotope ratios.

$$R_D = R_{Cor} \times \delta_{Cert} \times \delta_{Run} + \delta_{Blank} \qquad \textbf{Eq. (1)}$$

Where R_D is the final ratio, R_{Cor} is the blank and mass bias corrected ratio, δ_{Cert} is the uncertainty on the isotopic abundance of the mass bias based standard on IUPAC values, δ_{Run} is the variability of the mass bias ratio across the run, and δ_{Blank} is the uncertainty associated with blank subtraction.

Isotope Ratio Modeling

The change in isotope ratios for Ti during irradiation was modeled very simplistically using the Oak Ridge Isotope Generation (ORIGEN) code[43] (version 6.2, located within the ORNL Standardized Computer Analyses for Licensing Evaluation [SCALE] code[44]), designed to calculate time-dependent isotopic concentrations during and after irradiation for a complete set of nuclides produced by nuclear irradiation (including neutron activation). A 100 d, 0.96, 4.96. 15.13, and 20.00 y irradiation of a 1.0 g natural Ti target was modeled using a flux of 1.55×10^{14} $n \cdot cm^{-2} \cdot s^{-1}$ and a pneumatic tube-1 (PT-1) energy spectrum employing a thermal neutron shield, commonly used for irradiation in ORNL's neutron activation analysis (NAA) laboratory. These ratios were used for predicted model behavior only and are not representative of real samples or reactors.

Sample Preparation

Reagents were prepared in an International Organization for Standardization (ISO) Class 6 cleanroom. Samples and controls were prepared in the acid used for preconditioning/loading in leached perfluoro alkoxy (PFA) vials. CRM samples were prepared from a master stock of IRMM 183 and/or IRMM 86, with final concentrations of 20 ng g^{-1} and 1.5 pg g^{-1} for U and Pu, respectively. The valence state of Pu, in samples containing Pu, was adjusted to Pu(IV) as previously described.[24, 25] After separation, fractions were dried down and dissolved in 2% HNO_3 (1.5 mL). When necessary, the final sample was aliquoted for analysis as follows: 0.5 mL by ICP-SFMS, 0.5 mL by MC-ICP-MS, and 0.5 mL diluted to 5 mL (2% HNO_3) for ICP-OES analysis.

Graphite samples were prepared by ashing the graphite pellet in a quartz crucible in a Thermcraft tube furnace (Winston Salem, NC) equipped with a Eurotherm 2404 temperature controller (Ashburn, VA) at 850 °C until ashing was complete (~48 h). The resulting ash residue was quantitatively transferred and digested in 3.6 M HNO_3–2.5 M HF (11 mL) for 48 h at 125 °C followed by 30% H_2O_2 (1 mL) and 4 M HNO_3 (3 mL) for 48 h at 50 °C with dry down steps between reagent additions. Three archived graphite samples, that were previously digested and had known values for U and Pu isotope ratios, were used for final method validation. To ensure all Pu was in solution, 0.1 mL conc. HF was added to each archived sample and the sample was heated at 100 °C overnight.[24] Archived samples were dried down and reconstituted in 3 mL of 3M HNO_3

prior to separation. After separation, samples were dried down and dissolved in 2% HNO_3 and submitted for isotopic analysis by MC-ICP-MS.

Column Separations Method

The full separation scheme for U, Pu, and Ti is detailed in Table 1. The separation of U and Pu using stacked 1 mL TEVA/UTEVA cartridges was carried out as previously described.[24, 25] The effluent from the sample load, vial rinse, and stacked cartridge rinse (Steps 4-6) were collected for further Ti separation. The dried effluent, from Steps 4-6, was dissolved in 12 M HNO_3 for the separation of Ti on DGA-normal (DGA) followed by Anion Exchange, 1-X8 (IX) based loosely on work by Zhang et. al.[34] As the 2 mL cartridges are significantly larger than previously used columns[34], some initial method design was evaluated to determine the eluent volumes necessary for complete Ti recovery from each resin.

Table 1. Separation scheme outline for the separation of U, Pu, and Ti adapted from previous work.[24, 25, 34]

Step	Description	Vol (mL)	Reagent	Destination
Rinse exterior of TEVA/UTEVA cartridge with water				
1	UTEVA Clean	3	0.01 M HNO_3	Discard
2	UTEVA Precondition	5	3 M HNO_3	
3	TEVA Precondition	5	3 M HNO_3	
Stack cartridges, TEVA over UTEVA				
4	Load Sample	3	3 M HNO_3	Ti Fraction
5	Rinse Sample Vial	3	3 M HNO_3	
6	Wash Stacked Cartridges	10	3 M HNO_3	
Separate cartridges, store TEVA cartridge upright, UTEVA cartridge attached				
7	Wash UTEVA Cartridge	5	3 M HNO_3	Discard
8	Elute U from UTEVA Cartridge	4.5	0.02 M HNO_3-0.005 M HF	U Iso analysis
Discard UTEVA cartridge, rinse syringe barrel with 3 mL 3 M HNO_3, TEVA cartridge attached				
9	Wash TEVA Cartridge	5	3 M HNO_3	Discard
10	Wash TEVA Cartridge	3	9 M HCl	
11	Elute Pu from TEVA Cartridge	10	0.1 M HCl-0.06 M HF	Pu Iso Analysis
Dry down Ti Fraction from Steps 4-6 and dissolve in 2 mL of 12 M HNO_3				
Rinse exterior of DGA cartridge with water				
12	Clean	10	3 M HNO_3	Discard
13		10	3 M HNO_3 - 1 wt% H_2O_2	
14		4	H_2O	
15	Precondition	15	12 M HNO_3	
16	Load Sample	2	12 M HNO_3	
17	Rinse Sample Vial	10	12 M HNO_3	
18	Elute Ti	10	12 M HNO_3 - 1 wt% H_2O_2	Ti Fraction
Dry down Ti Fraction (Step 18) for further separation and dissolve in 2 mL of 4 M HF				
Rinse exterior of IX cartridge with water				

19	Clean	10	3 M HNO_3	Discard
20		2	H_2O	
21		6	0.4 M HCl – 1 M HF	
22		5	9 M HCl – 0.01 M HF	
23		5	H_2O	
24	Precondition	6	4 M HF	
25	Load Sample	2	4 M HF	
26	Rinse Sample Vial	10	4 M HF	
27	Wash Cartridge	10	0.4 M HCl – 1 M HF	
28	Elute Ti	10	9 M HCl – 0.01 M HF	Ti Iso Analysis

Safety and Hazards. Materials used in this work present radiological risks and should be handled appropriately.

Results and Discussion

Blanks and Ti Ratio Measurement Uncertainty

Process blanks for U and Pu using the method in Table 1 were within the uncertainty of previously reported values (< 60 pg U, < 15 fg Pu).[24, 25] To minimize the Ti process blanks, a larger IX resin column was used with smaller mesh size in comparison to previous work by Zhang et. al.[34] aimed at enhancing the number of reaction sites thereby increasing the column decontamination factor.[45, 46] The elution profile for Ti on the individual DGA and IX columns was verified by collecting 1 mL fractions during Ti elution using triple the eluent volume suggested by Zhang et. al.[34] Elution profiles and Ti recovery were in good agreement for the DGA resin with 10 mL yielding near quantitative (>99%) recovery based on ICP-OES results. However, the larger IX cartridge required twice the volume for quantitative elution (>98%) than previously reported.[34] Examination of reagent blanks from both DGA and IX columns determined on the Element 2 yielded 0.1 – 1 ng natural Ti total after separation through both columns which was significantly lower than previously reported values of 4 – 20 ng.[34] These values were above limit of quantification for Ti (0.1 ng), which was calculated at ten times the instrument blank for the SFMS divided by the slope of the calibration curve.

An important note is that much of the published Ti isotope data is from geological samples containing Ti in the μg g^{-1} range[27, 32, 37-39], whereas we report Ti data containing an order of magnitude less Ti (ng g^{-1}). This lower Ti quantity is more appropriate to nuclear grade graphite,

as it is expected that nuclear grade graphite will have significantly lower levels of trace impurities. However, it is thus necessary to understand the effect of Ti content on the overall measurement uncertainty. To better understand the significant components of the error budget, a single element Ti standard from High Purity Standards at 10 μg g^{-1} was diluted to make a calibration curve from 1 – 200 ng g^{-1}. The isotopic ratios for Ti in the calibration curve were then measured by MC-ICP-MS and the percent relative standard deviation (%RSD) of the isotope ratio measurement is reported in Table 2. The calibration curve demonstrates a high %RSD (>1%) for samples containing ≤ 25 ng g^{-1} and no significant increase in precision was noted above 50-100 ng g^{-1}. While the measurement of the isotopic ratio is still possible at low concentrations (<10 ng g^{-1}), the associated uncertainty in the measurement will be larger than a similar sample with higher Ti content.

Table 2. Compilation of the %RSD for the Ti isotope ratios as measured by MC-ICP-MS at different concentrations of natural Ti.

Conc (ng g^{-1})	$^{46}Ti/^{48}Ti$	$^{47}Ti/^{48}Ti$	$^{49}Ti/^{48}Ti$	$^{50}Ti/^{48}Ti$
1	9.3	19	21	16
5	1.9	2.3	3.4	4.1
10	1.6	2.0	1.2	1.3
25	0.85	0.57	0.92	1.0
50	0.76	0.62	0.75	0.83
100	0.74	0.54	0.76	0.78
150	0.74	0.54	0.75	0.77
200	0.74	0.54	0.74	0.77

The uncertainty of the Ti isotope ratio measurements was evaluated using the GUM Workbench® to estimate the result and calculate the expanded uncertainty based on input quantities into the mathematical model (Eq. 1). GUM Workbench® further calculates an uncertainty budget which displays the percent contribution to the combined uncertainty for each input parameter. For the measurement of Ti isotope ratios, the uncertainty in the measured ratio (based on instrument response/counts) and the uncertainty associated with the isotopic ratios of the standards used for mass bias corrections were the only significant contributors (>0.1% of total) to the expanded uncertainty. Figure 1 shows the percent contribution to the uncertainty from these two quantities as the concentration of Ti was varied. At low Ti concentrations (< 10 ng g^{-1}) the primary contribution was from the MC-ICP-MS measurement of the ratio with little contribution from the uncertainty on the IUPAC ratios. As the Ti concentration increases (>25 ng g^{-1}) the

primary contribution shifts to the uncertainty associated with the IUPAC values for the Ti mass bias correction.[35] As such, any improvement to the overall uncertainty will require a Ti isotopic reference material with lower uncertainties which is currently unavailable. The need for U and Pu isotopic standards with lower uncertainties has also been communicated in prior studies.[47]

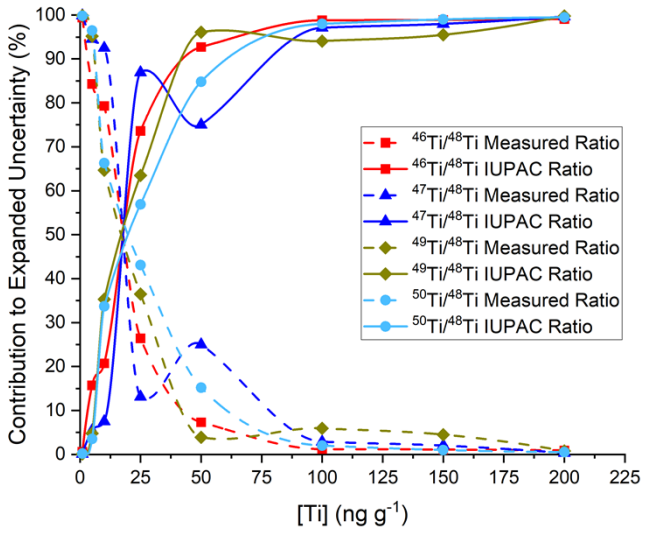

Figure 1. Contribution of the uncertainties associated with the measured and certified ratio to the expanded uncertainty of the measured ratio.

Ti Separation on DGA and IX Columns

To obtain the highest accuracy for the measurement of Ti ratios, it is necessary to obtain the greatest decontamination factor between trace metals relative to Ti. This was investigated using a synthetic sample containing 61 trace elements (2 mL of 5 µg g^{-1} High Purity Standards 68B-A and 68B-B for a total of 10 µg of each element). As the interaction of these trace elements with TEVA and UTEVA resins has been reported[24, 25, 48, 49], triplicate samples were separated using the method outlined in Table 1 for the DGA and IX columns only. The sample load, wash, and elution steps for the DGA resin (steps 16-18) and the sample rinse and elution steps for the IX resin (steps 27 and 28) were collected in 1 mL fractions and analyzed by OES and SFMS by external calibration. As expected from previously published data[34], the initial DGA column separated most trace elements (>90%) in the load and wash steps, while some carryover of Mo (68%) and Ca (35%) was observed. Additionally, carryover of Ag (10%) and Sn (6%) was also found in the Ti fraction after separation on the DGA column. The remaining elements demonstrated less than 0.5% (50 ng) carry over. Continued separation of the Ti fraction on the IX column significantly improved

the separation with carryover of Ca and Mo < 2%, Ag <1% and Sn < 0.1% suggesting an overall decontamination factor for the full procedure of better than 98% in a sample containing equivalent concentration of concomitant elements relative to Ti. Analysis of the Ti isotope ratios in the final separated fraction demonstrated results with expanded uncertainties that encompassed the isotope ratios for natural Ti as expected. This suggests that the remaining trace elements in the purified Ti fraction did not interfere with the MC-ICP-MS measurement. When extrapolated to samples with lower concentrations of trace impurities, it is expected that these elements will also not interfere with the Ti isotopic measurement.

Additionally, to verify that the IX and DGA columns would not perturb the measured isotopic distribution of a Ti sample, an enriched ^{47}Ti stable isotope spike was separated using the column procedure and the isotope ratios examined after separation. It was important to use an enriched sample since irradiation models of Ti suggest significant deviations from natural isotope ratios. For example, using a simple model in ORIGEN, after a 4.96 y irradiation the ^{46}Ti/^{48}Ti ratio would be 0.1126 and the ^{47}Ti/^{48}Ti ratio would be 0.1014 compared to 0.1119 and 0.1009, respectively, for natural Ti. Triplicate samples of the enriched ^{47}Ti stock (~2.5 μg g^{-1}) were separated successfully using the separation scheme presented in Table 1. As the enriched ^{47}Ti spike is not a CRM, the unseparated spike was also measured in triplicate in the same MC-ICP-MS run with the samples at a similar instrument response. Samples were screened prior to isotope ratio measurement on the MC-ICP-MS and showed no significant presence of the common interference elements (^{44}Ca, ^{51}V, and ^{52}Cr) in medium resolution mode. Average sample results by MC-ICP-MS were in good agreement with the average unseparated enriched spike as shown in Table 3.

Table 3. Average Ti isotope ratios with the expanded uncertainties (U_C) for an enriched ^{47}Ti spike with and without DGA/IX column purification.

	^{46}Ti/^{48}Ti	**U_C**	**^{47}Ti/^{48}Ti**	**U_C**	**^{49}Ti/^{48}Ti**	**U_C**	**^{50}Ti/^{48}Ti**	**U_C**
Ave. Spike	0.0769	0.0012	20.57	0.11	0.03940	0.00054	0.03487	0.00046
Ave. Sample	0.0757	0.0023	20.50	0.11	0.03979	0.00084	0.03531	0.00049

Separation of U, Pu and Ti

Final method development was done in triplicate with simulated samples containing U (CRM IRMM 183, 20 ng g^{-1}), Pu (CRM IRMM 86, 1.5 pg g^{-1}), and Ti (^{47}Ti enriched spike, 500

ng g^{-1}) and the full method outlined in Table 1. The major $^{235}U/^{238}U$ and $^{240}Pu/^{239}Pu$ isotope ratios and minor $^{236}U/^{238}U$ and $^{234}U/^{238}U$ isotope ratios were all in excellent agreement with certified values as shown in Table 4. The minor $^{241}Pu/^{239}Pu$ and $^{242}Pu/^{239}Pu$ isotopic ratios in the CRM are of low abundance 2.5×10^{-4} and 7.6×10^{-5}, respectively, and therefore were not used for comparison. As the ^{47}Ti isotope spike is not a CRM, the spike solution was measured before and after separation for comparison at similar instrument response. Table 5 displays the average isotope ratio measurement for Ti and showed no significant differences. Three blanks were also run with these samples and demonstrated no cross contamination of U, Pu, or Ti. Samples were consistent with previously reported blank values for U and Pu[24, 25] and Ti showed < 1 ng total for the reagent blanks.

Table 4. Average U and Pu isotope ratio and expanded uncertainties (U_C) as measured by MC-ICP-MS from simulated U/Pu/Ti samples.

Ratio	$^{234}U/^{238}U$	U_C	$^{235}U/^{238}U$	U_C	$^{236}U/^{238}U$	U_C	$^{240}Pu/^{239}Pu$	U_C
CRM	0.000019755	0.000000022	0.0032157	0.0000016	0.000148358	0.000000054	0.0224340	0.0000051
Ave. Sample	0.00001984	0.00000019	0.0032113	0.0000033	0.0001493	0.0000015	0.02235	0.00063

Table 5. Average Ti isotopic ratios and expanded uncertainties (U_C) as measured by MC-ICP-MS from simulated U/Pu/Ti samples.

Ratio	$^{46}Ti/^{48}Ti$	U_C	$^{47}Ti/^{48}Ti$	U_C	$^{49}Ti/^{48}Ti$	U_C	$^{50}Ti/^{48}Ti$	U_C
Ave. Spike	0.067	0.012	19.6	1.9	0.0377	0.0031	0.0329	0.0027
Ave. Sample	0.0709	0.0066	19.6	1.1	0.0393	0.0033	0.039	0.014

Three samples of Alabama Graphite (AG Lot: 2017-1) were ashed and digested with the goal of determining U, Pu, and Ti isotope ratios using the full separation protocol. After ashing and acid digestion, a fraction of the graphite sample (~60%) was separated following the method outlined in Table 1. Isotope ratio data for U and Ti, in all three samples, were in excellent agreement with each other within the uncertainty of the analysis. As these samples were not doped with a Pu CRM for quality control purposes, no Pu was present in these natural graphite samples and Pu isotope ratio measurements are not reported. The U content ranged between the three samples but demonstrated isotope ratios with the expected natural abundance. The measured Ti isotope ratios also showed natural abundance. While the amount of Ti present in these samples

was not quantified, as the primary focus of this work is the analysis of Ti isotope ratios, there was significantly more signal associated with these samples than with samples analyzed previously suggesting Ti is present in significant (μg) quantities.

The separation of archived graphite samples from a past interlaboratory comparison exercise was successfully achieved using the method in Table 1. The three samples had previously reported values for U and Pu isotopics and content for comparison. As the concentration of samples can change over time during archiving, samples were only analyzed for isotope ratios.[24, 25] These were in excellent agreement with the previously reported values as shown in Table 6. The $^{234}U/^{238}U$ for Graphite 2 was 8% low in comparison to the previous value. As the samples were several years old at the time of current processing, it is difficult to determine the cause of this discrepancy; however, it is not attributed to the method as the process blanks and other samples run in conjunction with Graphite 2 were not contaminated. Additionally, the other U isotope ratios for Graphite 2 were in excellent agreement with previously determined values, making contamination unlikely.

Table 6. Comparison of measured vs. reported values with expanded uncertainties (U_C) for major and minor U isotopic ratios and major Pu isotopic ratios for archived graphite samples.

Measured/Reported	**$^{234}U/^{238}U$**	**U_C**	**$^{235}U/^{238}U$**	**U_C**	**$^{236}U/^{238}U$**	**U_C**	**$^{240}Pu/^{239}Pu$**	**U_C**
Graphite 1	100.4%	1.7%	99.7%	1.1%	101.6%	1.5%	100.0%	6.0%
Graphite 2	92.4%	1.2%	99.4%	1.1%	100.9%	1.6%	100.5%	1.3%
Graphite 3	100.3%	2.3%	99.9%	1.1%	98.3%	2.4%	99.9%	1.7%

Ti isotope ratio measurements for the three Alabama Graphite samples and three interlaboratory comparison graphite samples are displayed in Figures 2 and 3. Of the three archived samples, one sample had unperturbed Ti ratios, and the remaining two demonstrated perturbed isotopics when compared to natural Ti abundances. This was expected as two of the three archived graphite samples had been irradiated. The three archived graphite samples contained various amounts of Ti in the final separated fractions, but all three samples had significantly less than the amount present in the Alabama Graphite. It is interesting to note the effect of neutron capture on the isotope ratios for Ti when compared to natural abundances. As ^{46}Ti and ^{50}Ti have the smallest neutron cross section, the abundance of these two isotopes should change the least. However, the ^{47}Ti, ^{49}Ti, and especially ^{48}Ti will undergo thermal (n,γ) reactions to form additional ^{48}Ti, ^{50}Ti, and

^{49}Ti respectively. While some variation was observed in the ^{46}Ti/^{48}Ti and ^{47}Ti/^{48}Ti isotope ratios as shown in Figure 2, they were not significantly different than natural ratios (within 3σ) and the shift in isotope ratios was in the same direction as the irradiated model Ti. As expected, a significant difference in the ^{49}Ti/^{48}Ti and ^{50}Ti/^{48}Ti ratios was observed for the (n,γ) reactions with thermal neutrons as shown in Figure 3. Additionally, the ^{49}Ti/^{48}Ti and ^{50}Ti/^{48}Ti ratios did shift in the same general direction as the model. The deviating behaviors are explained by differences in the irradiation neutron energy spectrum and in the total fluence of the model compared to expected nuclear graphite conditions. It is also interesting to note a significant difference in the isotope ratios of the two irradiated samples (Graphite 1 and Graphite 2) suggesting different environments during irradiation (i.e., positioning or time in the reactor) for these samples.

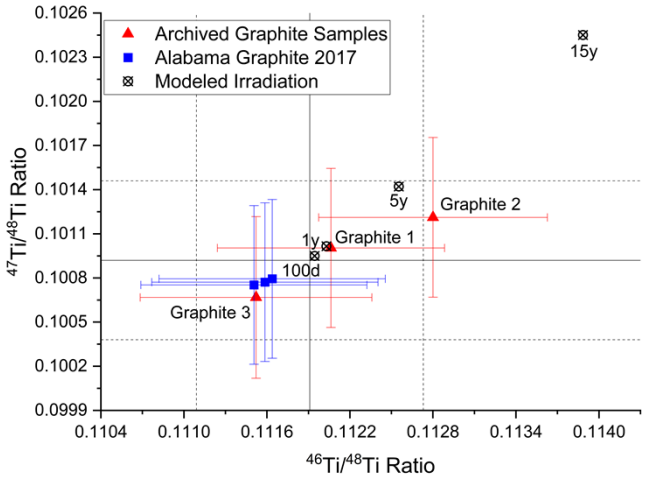

Figure 2. Comparison of the sample sets, with expanded uncertainties, to natural Ti isotope ratios (solid black line) and uncertainties (dashed black line) and the modeled irradiated ^{46}Ti/^{48}Ti and ^{47}Ti/^{48}Ti ratios.

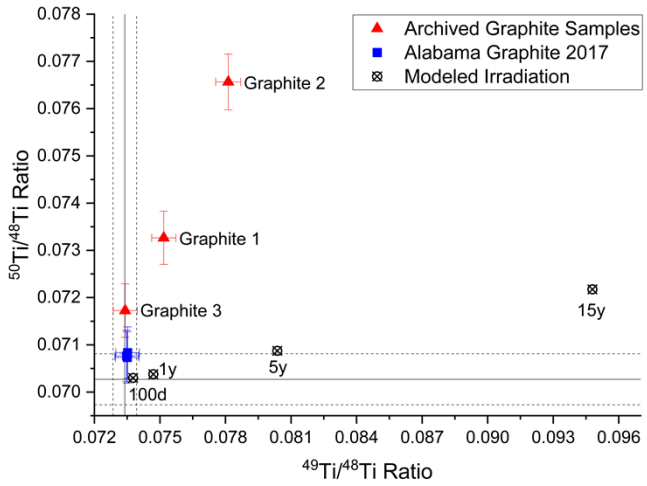

Figure 3. Comparison of the sample sets, with expanded uncertainties, to natural Ti isotope ratios (solid black line) and uncertainties (dashed black line) and the modeled irradiated $^{49}Ti/^{48}Ti$ and $^{50}Ti/^{48}Ti$ ratios.

Conclusions

The work presented herein exhibits the effective isolation, purification, and isotopic analysis of U, Pu, and Ti from a suite of various graphite samples. The separation and purification were achieved using four different commercially available Eichrom™ prepacked cartridges: TEVA, UTEVA, DGA-normal, and Anion Exchange (1-X8). The selected resin cartridges provided a means for excellent removal of spectral interferences enabling the accurate and precise isotope ratio measurement of U, Pu, and Ti by MC-ICP-MS. Ultimately, the precision of MC-ICP-MS Ti measurements was limited by the uncertainties associated with the currently available CRMs. Despite this uncertainty, purification of CRM samples was effective and measured isotope ratios were in good agreement with certified values. The separation of U, Pu, and Ti from Alabama Graphite was achieved in triplicate, and results indicated natural isotope abundance ratios for Ti and U. Three samples of nuclear grade graphite were also successfully separated using this method. Isotope ratio analysis of the U and Pu in the nuclear graphite was overall in excellent agreement with previously reported results. Analysis of the Ti isotope ratios from the three nuclear grade graphite samples demonstrated significant differences in the Ti ratios which suggests that two of

the samples had been previously irradiated. Overall, the separation method described herein is fully capable of separating U, Pu, and Ti from very complex matrices, while producing purified fractions that preclude the need for post-measurement interference corrections.

Conflicts of Interest

There are no conflicts of interest to declare.

Acknowledgements

This work is supported by the Department of Energy's National Nuclear Security Administration under contract DE-AC-05-000R22725 with UT–Battelle, LLC. Oak Ridge National Laboratory is managed by UT–Battelle for the Department of Energy under Contract DE–AC05–000R22725.

Notes

References

1. National Minerals Information Center, Graphite Statistics and Information, https://www.usgs.gov/centers/nmic/graphite-statistics-and-information, (accessed Mar 02, 2020).
2. D. E. Baker, *Nucl. Eng. Des.*, 1971, **14**, 413-444.
3. M. Gill, F. Livens and A. Peakman, in *Future Energy (Second Edition)*, ed. T. M. Letcher, Elsevier, Boston, 2014, DOI: https://doi.org/10.1016/B978-0-08-099424-6.00009-0, pp. 181-198.
4. R. Rhodes, *The Making of the Atomic Bomb*, Simon and Schuster, New York, NY, 2012.
5. R. Plukienė, E. Lagzdina, L. Juodis, A. Plukis, A. Puzas, R. Gvozdaitė, V. Remeikis, Z. Révay, J. Kučera, D. Ancius and D. Ridikas, *Radiocarbon*, 2018, **60**, 1861-1870.
6. H. S. Mahanti and R. M. Barnes, *Anal. Chem.*, 1983, **55**, 403-405.
7. K. Watanabe and J. Inagawa, *Analyst*, 1996, **121**, 623-625.
8. W. Bögershausen, R. Cicciarelli, B. Gercken, E. König, V. Krivan, R. Müller-Käfer, J. Pavel, H. Seltner and J. Schelcher, *Fresenius. J. Anal. Chem.*, 1997, **357**, 266-273.
9. M. Watanabe and A. Narukawa, *Analyst*, 2000, **125**, 1189-1191.
10. C. Pickhardt and J. S. Becker, *Fresenius. J. Anal. Chem.*, 2001, **370**, 534-540.
11. A. V. Bushuev, V. N. Zubarev and I. M. Proshin, *Atomic Energy*, 2002, **92**, 331-335.
12. A. Zacharia, S. Gucer, B. Izgi, A. Chebotarev and H. Karaaslan, *Talanta*, 2007, **72**, 825-830.
13. J. Datta, D. P. Chowdhury and R. Verma, *J. Radioanal. Nucl. Chem.*, 2014, **300**, 147-152.
14. S. M. Cruz, L. Schmidt, F. M. Dalla Nora, M. F. Pedrotti, C. A. Bizzi, J. S. Barin and E. M. M. Flores, *Microchem. J.*, 2015, **123**, 28-32.
15. A. Puzas, V. Remeikis, Z. Ezerinskis, P. Serapinas, A. Plukis and G. Duskesas, *Lith. J. Phys.*, 2010, **50**, 445-449.
16. J. S. Becker, C. Pickhardt and H.-J. Dietze, *Int. J. Mass Spectrom.*, 2000, **202**, 283-297.
17. A. D. Shinde, R. Acharya, R. Verma and A. V. R. Reddy, *J. Radioanal. Nucl. Chem.*, 2012, **294**, 409-412.
18. M. Ghosh, K. K. Swain, P. S. Remya Devi, T. A. Chavan, A. K. Singh, M. K. Tiwari and R. Verma, *Appl. Radiat. Isot.*, 2017, **128**, 210-215.
19. C. Pan and F. L. King, *Appl. Spectrosc.*, 1993, **47**, 300-304.
20. J. McNeece, B. Reid and T. Wood, *The Graphite Isotope Ratio Method (GIRM): A Plutonium Production Verification Tool*, Report PNNL-12095; TRN: US0904442 United States 10.2172/967298 TRN: US0904442 PNNL English, ; Pacific Northwest National Lab. (PNNL), Richland, WA (United States), 1999.
21. L. Yang, *Mass Spectrom. Rev.*, 2009, **28**, 990-1011.
22. S. Boulyga, S. Konegger-Kappel, S. Richter and L. Sangely, *J. Anal. At. Spectrom.*, 2015, **30**, 1469-1489.
23. S. F. Boulyga, A. Koepf, S. Konegger-Kappel, Z. Macsik and G. Stadelmann, *J. Anal. At. Spectrom.*, 2016, **31**, 2272-2284.
24. S. C. Metzger, K. T. Rogers, D. A. Bostick, E. H. McBay, B. W. Ticknor, B. T. Manard and C. R. Hexel, *Talanta*, 2019, **198**, 257-262.
25. S. C. Metzger, B. W. Ticknor, K. T. Rogers, D. A. Bostick, E. H. McBay and C. R. Hexel, *Anal. Chem.*, 2018, **90**, 9441-9448.

26. S. K. Aggarwal, *Anal. Methods*, 2016, **8**, 942-957.
27. I. Leya, M. Schönbächler, U. Wiechert, U. Krähenbühl and A. N. Halliday, *Int. J. Mass Spectrom.*, 2007, **262**, 247-255.
28. T. W. May and R. H. Wiedmeyer, *At. Spectrosc.*, 1998, **19**, 150-155.
29. S. F. Boulyga, C. Testa, D. Desideri and J. S. Becker, *J. Anal. At. Spectrom.*, 2001, **16**, 1283-1289.
30. S. A. Ansari and P. K. Mohapatra, *J. Chromatogr. A*, 2017, **1499**, 1-20.
31. J. Veliscek-Carolan, *J. Hazard. Mater.*, 2016, **318**, 266-281.
32. A. Makishima, X.-K. Zhu, N. S. Belshaw and R. K. O'Nions, *J. Anal. At. Spectrom.*, 2002, **17**, 1290-1294.
33. X. K. Zhu, A. Makishima, Y. Guo, N. S. Belshaw and R. K. O'Nions, *Int. J. Mass Spectrom.*, 2002, **220**, 21-29.
34. J. Zhang, N. Dauphas, A. M. Davis and A. Pourmand, *J. Anal. At. Spectrom.*, 2011, **26**, 2197-2205.
35. J. Meija, B. Coplen Tyler, M. Berglund, A. Brand Willi, P. De Bièvre, M. Gröning, E. Holden Norman, J. Irrgeher, D. Loss Robert, T. Walczyk and T. Prohaska, *Pure Appl. Chem.*, 2016, **88**, 293.
36. K. Shuai, W. Li and H. Hui, *Anal. Chem.*, 2020, **92**, 4820-4828.
37. M.-A. Millet and N. Dauphas, *J. Anal. At. Spectrom.*, 2014, **29**, 1444-1458.
38. A. M. Davis, J. Zhang, N. D. Greber, J. Hu, F. L. H. Tissot and N. Dauphas, *Geochim. Cosmochim. Acta*, 2018, **221**, 275-295.
39. K. K. Larsen, D. Wielandt and M. Bizzarro, *J. Anal. At. Spectrom.*, 2018, **33**, 613-628.
40. G. Bucher and F. Auger, *J. Anal. At. Spectrom.*, 2019, **34**, 1380-1386.
41. B. T. Manard, S. C. Metzger, K. T. Rogers, B. W. Ticknor, D. A. Bostick, N. A. Zirakparvar and C. R. Hexel, *Int. J. Mass Spectrom.*, 2020, **455**, 116378.
42. *Evaluation of measurement data – Guide to the expression of uncertainty in measurement JCGM 100:2008 (GUM 1995 with minor corrections)*, Report JCGM 100:2008, BIPM Joint Committee for Guides in Metrology, Paris, 2008.
43. B. T. Rearden, Oak Ridge National Laboratory SCALE Website, https://www.ornl.gov/scale/overview).
44. I. C. Gauld, G. Radulescu, G. Ilas, B. D. Murphy, M. L. Williams and D. Wiarda, *Nucl. Technol.*, 2011, **174**, 169-195.
45. J. S. Becker, in *Handbook of Radioactivity Analysis (Third Edition)*, ed. M. F. L'Annunziata, Academic Press, Amsterdam, 2012, DOI: https://doi.org/10.1016/B978-0-12-384873-4.00013-X, pp. 833-870.
46. C. Hill, in *Advanced Separation Techniques for Nuclear Fuel Reprocessing and Radioactive Waste Treatment*, eds. K. L. Nash and G. J. Lumetta, Woodhead Publishing, 2011, DOI: https://doi.org/10.1533/9780857092274.3.311, pp. 311-362.
47. K. J. Mathew, F. E. Stanley, M. R. Thomas, K. J. Spencer, L. P. Colletti and L. Tandon, *Anal. Methods*, 2016, **8**, 7289-7305.
48. E. P. Horwitz, M. L. Dietz, R. Chiarizia, H. Diamond, A. M. Essling and D. Graczyk, *Anal. Chim. Acta*, 1992, **266**, 25-37.
49. E. P. Horwitz, M. L. Dietz, R. Chiarizia, H. Diamond, S. L. Maxwell and M. R. Nelson, *Anal. Chim. Acta*, 1995, **310**, 63-78.